GAMBE: multipurpose sandwich detector for neutrons and photons

A. Ahmed[a], S. Burdin[a], G. Casse[a], van Zalinge[b], S. Powel[a], J. Rees[a], A. Smith[a], and I. Tsurin[a]

[a]University of Liverpool, Faculty of Science and Engineering, Department of Physics, Oxford Street, Liverpool, UK, L69 7ZE
[b]University of Liverpool, Faculty of Science and Engineering, Department of Electrical Engineering and Electronics, Brownlow Hill Street, Liverpool, UK, L69 3GJ

ABSTRACT

Detectors made with semiconductors such as silicon can be efficiently used for detecting and imaging neutrons when coated with suitable materials. They detect the charged reaction products resulting from the interaction of thermal neutrons with materials with high capture cross section like ^{10}B, ^{6}Li, and ^{6}LiF. This work describes the performance of a thermal neutron detector system, GAMBE, which is based on silicon sensors and a layer of neutron-sensitive material, such as a lithium fluoride film or a lithium-6 foil, in a sandwich configuration. This arrangement has a total detection efficiency of 4 ± 2 %, 7 ± 1 %, $and 12 \pm 1$ % for 7 μm ^{6}LiF film, 40 μm and 70 μm ^{6}Li foil respectively. Also, it enhances the rejection of fake hits using a simple coincidence method. The coincidence that defines a true neutron hit is the simultaneous signal recorded by the two sensors facing the conversion layer (or foil). These coincidences provide a very good method for rejecting the spurious hits coming from gamma-rays, which are usually present in the neutron field under measurement. The GAMBE system yields a rejection factor at the level of 10^8 allowing very pure neutron detection in high gamma background conditions. However, the price to pay is a reduction of the detection efficiency of 1 ± 1 % or 0.9 ± 0.3 % for 7 μm ^{6}LiF film and 40 μm ^{6}Li foil respectively.

Keywords: Neutron detector, Semiconductor detector, Neutron detection, Neutron conversion

1. INTRODUCTION

A neutron is a neutral particle which cannot interact with matter by means of Coulomb force, which forms an energy loss mechanism for charged particles and electrons. Also, neutrons can travel through many centimeters of matter without any interaction and therefore, can be totally unseen by a conventional detector.[1]

The neutron interacts with the nucleus of the conversion material and as a result of this interaction, the neutron may produce secondary radiation, or the energy and direction of the neutron change significantly. Secondary radiation arising from the interaction of a neutron with the conversion material are mainly heavy charged particles. These particles can be produced by neutron-induced nuclear reactions, or they may result from the nuclei of the absorbing material itself, which gain enough energy from the collision with a neutron. Therefore, the detection of the neutrons depends on this secondary radiation, and most neutron detectors utilize some materials with a large absorption cross section depending on neutron energy for conversion of an incident neutron into secondary charged particles, which can be detected directly using an appropriate detector.[2,3]

There are different types of materials which are used as a converter in thermal neutrons detection; these materials have a large absorption cross section for high detection efficiency, and the reaction products must have the capability to leave the material with positive detection energies. The isotopes ^{6}Li, ^{10}B, and ^{157}Gd have such features and are serious candidates as a neutron converter.[4]

For ^{6}Li, the thermal neutron (0.0259 eV) absorption cross section (σ) is 940 b, which is a relatively high value. However, this value decreases as the neutron energy increases, with an inverse proportion to neutron velocity over much of the energy range.[5] ^{6}Li could be used in the pure form as a neutron reactive material although it demands cumbersome handling procedures because of its corrosiveness and reactivity.[6]

Further author information: (Send correspondence to A. Ahmed and S. Burdin)
A. Ahmed: E-mail: m.o.ahmed@liv.ac.uk, Telephone: +44 (0)7710517430
S. Burdin : E-mail: s.burdin@liv.ac.uk, Telephone: +44 (0)7791859200

The primary reaction of neutron interactions is $^{6}Li(n,\alpha)^{3}H$; this reaction produces an alpha particle (at 2.05 MeV) and a triton (at 2.73 MeV) in opposite directions with total Q-value of 4.78 MeV. Although ^{6}Li has a smaller thermal neutron absorption cross section than ^{10}B and ^{157}Gd, the higher energy reaction products make it attractive for thermal neutron detection. Furthermore, the low atomic density and the low mass density of ^{6}Li result in a large reaction product range exceeding the ranges of the reaction products for ^{10}B film, with a sufficient range for a triton $L_H = 126.77\ \mu m$ and an efficient range for alpha $L_\alpha = 19.05\ \mu m$.[7] Due to the chemical reactivity of pure ^{6}Li, it could alternatively be used in the form of ^{6}LiF, which is more stable, however, the range of reaction products will be affected with $L_H = 29.25\ \mu m$ and $L_\alpha = 4.64\ \mu m$.[7]

Semiconductor-based detectors such as a silicon sensor could be coupled with various converters to use as a neutron detector. Theses sensors offer valuable features, such as compactness and robustness, low weight, bias voltage, and battery consumption and a high count rate capability.[8] The high density of the semiconductor results in a compactness, because of the short ranges of the reaction products, but it also increases the probability of gamma-rays interaction. That suggests silicon as a best choice for neutrons detector because of the relatively low Z of silicon, which decreases gamma-rays interaction probability.[9] Also, the sensitivity to gamma rays is expected to be low in Si wafer thickness $(30 - 300\ \mu m)$ and by using electronic discrimination set up to 100 keV, which will electronically cut off the electrons produced by the gamma ray background.[10]

In this work, the feasibility of using enriched ^{6}Li with silicon sensors in a sandwich configuration as a thermal neutron counter has been investigated. Tests have been performed using ^{6}Li in a ^{6}LiF coating and in its pure metallic form as a foil. Lithium has a natural abundance of 92.5 % of ^{7}Li and 7.5 % of ^{6}Li, so the lithium (and ^{6}LiF) used as part of this study with enriched ^{6}Li at 95 %. The principle behind thermal neutron detection using thin-film coated semiconductor sensors described in ref.[11]

Thin layers of neutron reactive material applied to a semiconductor detector, such as a silicon radiation sensor and in the presence of thermal neutron, the reaction products measure by the semiconductor detectors. The reactive layer must be thin enough to allow reaction products to escape, but as high detection efficiency is required, the layer must be as thick as possible. A sandwich sensor configuration has been chosen for the detection of neutrons, with a reactive thin film between the two silicon sensors, which allows both reaction products to be detected. Detecting both reaction products in coincidence i.e. at the same time is investigated as a method of rejecting gamma-ray induced events in the detector.

2. SIMULATION

Simulations have been performed using Geant4[12] to identify the optimal film thickness. The sandwich detector geometry has been set up in the simulation and consists of two $12.5 \times 12.5\ mm^2$ silicon diodes which are assigned as A and B with a thickness of 300 μm, on either side of a sensitive film with an adjustable thickness.

There is also a 100 nm Al contact covering the active region of both silicon sensors. For the lithium foil simulations, there is a 0.3 mm argon gas layer which separated between the foil and both silicon diodes, and for the detector based on ^{6}LiF film a 0.3 mm layer of air is inserted between the film and one of both silicon sensors as shown in fig 1.

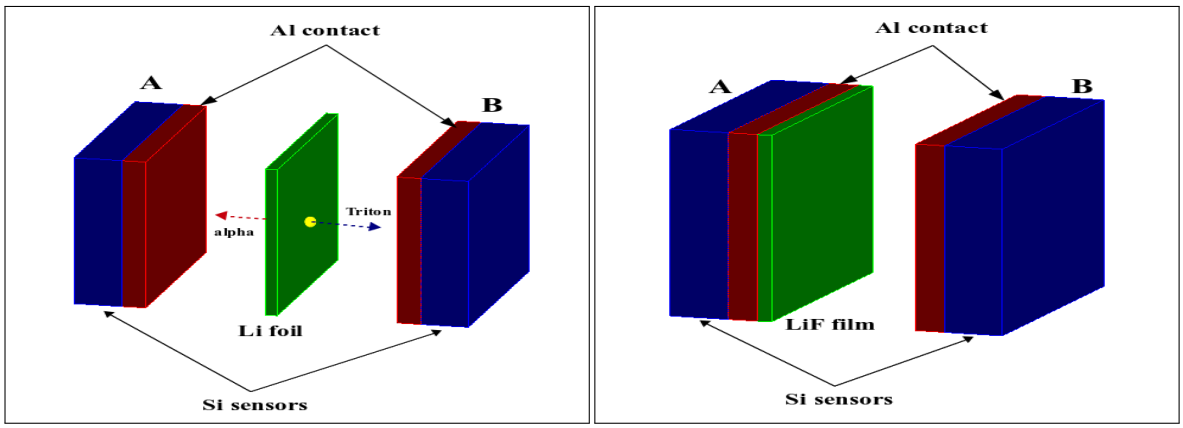

(a) ^{6}Li foil configuration. (b) ^{6}LiF film configuration.

Fig 1. GAMBE, thermal neutron detector consists of two Si sensors in a sandwich configuration.

For the simulation, each event begins with the generation of a random position within the sensitive film volume where a thermal neutron will be captured. From this point, one alpha is assigned an arbitrary direction with an energy of 2.05 MeV and a triton is assigned the opposite direction with an energy of 2.73 MeV. This model assumes that neutron capture is distributed uniformly within the converter film. This is a good approximation for the thickness range under investigation because the probability of a thermal neutron absorption would be constant over the entire area of the converter film.

For each event (alpha or triton), the energy deposited in each of the two silicon sensors is measured. If the energy of this event which could be detected by each of both diodes is above a threshold value of 100 keV; this counted as single event above threshold. Moreover, if this energy is detected by both sensors at the same time and it is greater than the predefined threshold value, this is counted as a coincidence event. To distinguish thermal neutron induced events from other causes, namely gamma-rays, a pulse-height discrimination is set up. Where the energy deposited in each of the two silicon detectors for each event is between 1.56 and 2.73 MeV, this is considered as a neutron conversion (NC) event with a sound energy pulse. If two events are counted at the same time, this is considered as a coincidence with sound energy pulse related to a neutron conversion event.

The thermal neutron detection efficiency, ε, of the detectors has been calculated using equation 1:

$$\varepsilon = \frac{n}{N} \times P(x) = \frac{n}{N} \times \{1 - exp(-\frac{N_A}{w_A} \times \rho \times \sigma \times x)\} \tag{1}$$

Where n is the number of detected events, N the total number of generated events, and $P(x)$ the probability of an incident thermal neutron being captured as a function of the reactive film thickness, x. N_A is Avogadro's number, w_A the atomic or molecular weight of the reactive film, ρ the density of the reactive film and σ the thermal-neutron cross-section for ^{6}Li is 940 b.

The simulated thermal neutron detection efficiency for a range of ^{6}LiF film and ^{6}Li foil responsive thicknesses is displayed at fig 2 which shows a different types of detection efficiencies depending on the criteria of how the efficiency has been calculated.

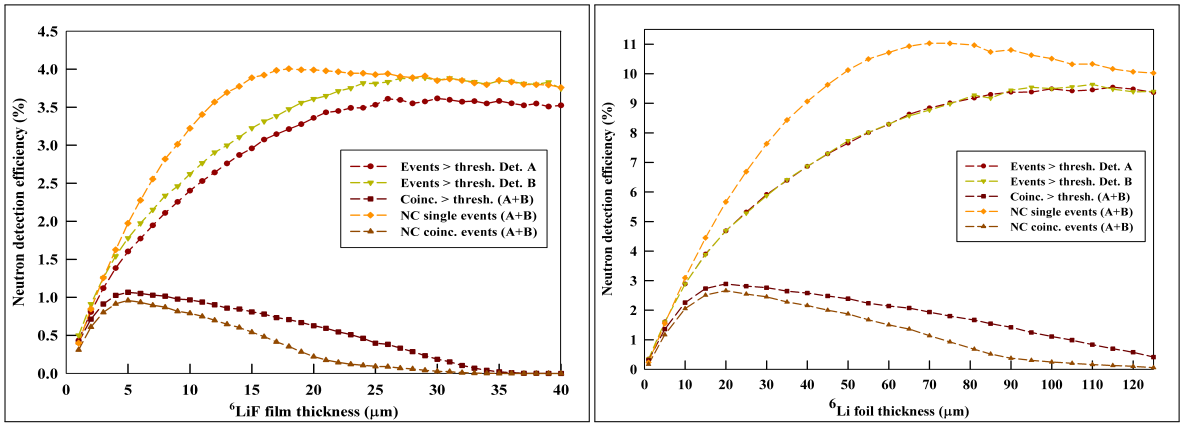

(a) ^{6}LiF film. (b) ^{6}Li foil.

Fig 2. The dependency of the neutron detection efficiency on the thickness of conversion material.

In addition to the detection efficiency of all coincidence events above a predefined threshold value. The detection efficiency is also presented for single events. These events are related to neutrons to be captured in the converter film producing particularly a triton with an energy in between 1.56 MeV to 2.73 MeV and identified as a neutron conversion single event. Furthermore, The detection efficiency of coincidence events which fall in that energy range is identified as a neutron conversion coincident events.

The simulations suggest the optimal film thickness of ^{6}LiF for measuring coincidences is approximately 5 μm but due to experimental limitation the film thickness of 7 μm was chosen to be examined practically. As the detection efficiency of coincidences is expected to change little between 5 and 10 μm.

The coincidence detection efficiency drops for greater values of the thickness, disappearing at approximately 35 μm. At the optimal thickness, nearly 32 % of the emitted alpha-triton pairs are detected in coincidence. The simulations propose as well, that 18 μm is suggested as the optimum film thickness with approximately 60 % of of the emitted alpha-triton pairs to be detected as a neutron conversion single event. Table 1 presents the total detection efficiency for both sensors (A+B) as well as the variation of different types of the detection efficiency with 5, 7 and 18 μm of ^{6}LiF film thickness.

Table 1. Neutron detection efficiency (%) as estimated from simulation for different thickness of ^{6}LiF films.

Film thickness	Total (A+B)	Coincidence	NC single events	NC coinc. events
5 μm	3.4	1.1	2	1
7 μm	4.1	1	2.6	0.9
18 μm	6.7	0.7	4	0.4

With respect to ^{6}Li foil, the simulations assert that the range of ^{6}Li foil thickness surpasses that of ^{6}LiF film for all variety of the neutron detection efficiencies. The optimum thickness for the detection of coincidence and neutron conversion single events is predicted to be 20 and 70 μm respectively. Due to experimental limitation, ^{6}Li foil of thickness 40 μm is chosen instead of 20 μm for experimental measurements. Table 2 demonstrates the total detection efficiency of both detector (A+B), in addition to the variety of neutron detection efficiencies with a ^{6}Li foil of thickness 20, 40 and 70 μm.

Table 2. Neutron detection efficiency (%) as estimated from simulation for different thickness of ^{6}Li foils.

Film thickness	Total (A+B)	Coincidence	NC single events	NC coinc. events
20 μm	9.4	2.9	5.7	2.7
40 μm	13.7	2.6	9.1	2.2
70 μm	17.6	1.9	11.03	1.1

In conclusion the simulations clarify that ^{6}LiF film and ^{6}Li foil in the sandwich detector configuration with silicon sensors of an active area of 1 cm^2 could be used efficiently for the detection of thermal neutrons comparable to other detectors. It could be concluded also from the simulations that the pure lithium foil is more efficient than ^{6}LiF film for the purpose of thermal neutron detection. However, the chemical reactivity limits the use of pure lithium-6.

3. EXPERIMENTAL WORK

3.1 Geometry and Neutron flux calculations.

The source of neutrons used for all measurements taken as part of this work is a 1Ci Am/Be source. Neutrons emitted as part of the reaction $Be(\alpha, n)C^*$. A 1Ci source of this type emits 2.6 million neutrons every second ranging in energy up to 11 MeV. The reaction $Be(\alpha, n)C^*$ will often lead to the emission of a 4.43 MeV gamma-ray from the excited C nucleus (typically for $50 - 75$ % of results) which is necessary for these measurements as it can lead to the deposition of energy in the silicon sensors of the neutron detector.

The measurements are taken using the Am/Be neutron source, the detector has been placed in a position, which is referred to here as the calibration position. In the calibration position, the Am/Be source is placed inside a water-filled tank, with 25 cm of water between the source and the end of the reservoir. The detector sensors are placed 50 cm from the wall of the container, at the same height as the source as presented in fig 3a.

The thermal neutron detection efficiency of the detector in different configurations has been estimated, by calculating the thermal neutron flux at the calibration position using ^{3}He detector tubes. The ^{3}He detector tubes are industry standard 5 cm diameter, 1 m length tubes, of pressure 2 atm, and operating at a high voltage of 1100 V. The neutron sensitivity of these detectors is 322 cps/nv (nv is thermal neutron flux, $neutrons/cm^2/s$). Approximately 3 cps/nv per cm active tube length assuming no degradation of performance over the lifetime of the detector.

The tube is 50 cm from the end of the neutron tank, and the 1 Ci Am/Be source 25 cm inside the water tank. Other detectors including a lithium glass scintillator have been used to characterize the variation in the neutron flux along the

length of the tube as presented in fig 3b which shows that the neutron flux at the center of the tube is 1.40 times greater than over the entire pipe.

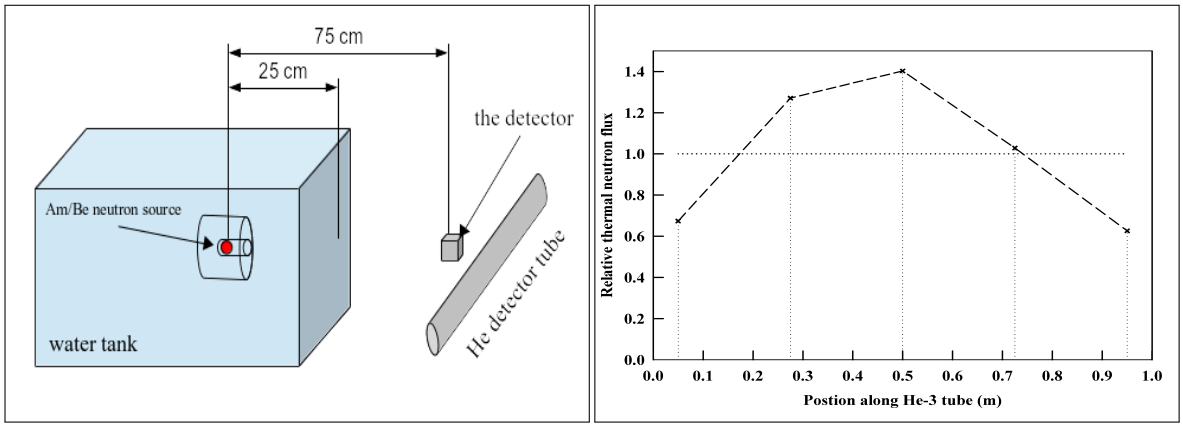

(a) calibration position. (b) neutron flux.

Fig 3. The geometry of calibration position of the detector and the variation of neutron flux along the ^{3}He tube.

^{3}He thermal neutron detector measured 232,745,950 counts over 229666-second corresponding to a detection rate of 1013.01 ± 0.07 cps, corresponding to a neutron flux at the calibration position of 4.4 nv. It is this figure that has been used to calculate the detection efficiency of the ^{6}LiF and ^{6}Li foil configurations of the GAMBE detector.

3.2 Detector configuration.

3.2.1 Bare sensor with no lithium.

Both silicon sensors have an active area of 1×1 cm^2 and are used in the sandwich configuration for counting events as a result of gamma-rays interaction with sensors resembling a thermal neutron. This detector used with the Am/Be neutron source at the calibration position and by placing the sensor in the sight of a ^{60}Co gamma-ray source with an activity of 30 kBq and a distance of 2 cm from a ^{60}Co source. These measurements are used for the calculation of the gamma rejection factor. Also, to show the ability of this GAMBE detector used in high background gamma field to discriminate between neutrons and gamma-ray interactions.

3.2.2 Si sensors with a LiF film coating.

A ^{6}LiF solution was prepared from 3 g of ^{6}LiF (Sigma-Aldrich 601411 95$\%$ enriched ^{6}Li) and ball milled in 20 cc ethanol. The ^{6}LiF solution mixed with 1 $\%$ PVP (MW 700000) solution with a ratio 1:1 was precipitated on the surface of the Si sensor (1.25×1.25 cm^2). A ^{6}LiF layer of 240 μg/mm^2 was applied to Si sensor to obtain a ^{6}LiF film with a thickness of about 7 μm on the surface of Si diode.

3.2.3 Si sensors with a pure Lithium foil.

Due to the highly reactive nature of lithium-6 metal, care was taken to maintain an inert environment for the lithium-6 foil to prevent corrosion. Lithium metal enriched up to 92 $\%$ ^{6}Li was cold-rolled into thin 40 and 70 μm foil using a stainless steel rolling apparatus inside an argon glove-box. The foil was mounted between the two silicon sensors while still inside the protective environment of the argon-filled enclosure of the glove-box and the entire sensor-lithium configuration was mounted within an airtight aluminum enclosure.

The simulations indicate that the optimal thickness of lithium-6 foil for observing alpha-triton coincidences is approximate 20 μm. However, it was not possible to achieve foil with a thickness less than 40 μm as any attempts to roll the foil to be thinner resulted in tears in the foil.

4. RESULTS AND DISCUSSION.

The Results presented here are for all measurements taken with the Am/Be neutron source in the calibration position for various sandwich detectors configuration in the following order:

1. Bare-sensor with no lithium.
2. ^{6}LiF film in a sandwich configuration with a thickness of 7 μm for the sensitive film.
3. ^{6}Li foil in a sandwich shapes with thicknesses of 40 and 70 μm.

4.1 GAMBE detection efficiency.

The calculated detection efficiencies for these different detector configurations using the total number of events observed in both sensors and the gross count of coincidence events are indicated in table 3.

Table 3: Neutron detection efficiency (%) for both ^{6}LiF film and ^{6}Li foil in a sandwich detector configuration.

Counted events				
Detector configuration	Total	Coinc.	NC single	NC coinc.
Bare Si sensors	37572	12229	262	27
^{6}LiF film 7 μm	11434	3856	4092	933
^{6}Li foil 40 μm	232697	48876	102199	12974
^{6}Li foil 70 μm	170025	11350	94557	1232
Neutron count rate (cps)				
Detector configuration	Total	Coinc.	NC single	NC coinc.
^{6}LiF film 7 μm	0.2±0.1	0.04±0.02	0.14±0.03	0.03±0.01
^{6}Li foil 40 μm	0.3±0.1	0.04±0.01	0.198±0.001	0.0251±0.0003
^{6}Li foil 70 μm	0.5±0.1	0.01±0.01	0.382±0.002	0.0047±0.0002
Neutron detection efficiency (%)				
Detector configuration	Total	Coinc.	NC single	NC coinc.
^{6}LiF film 7 μm	4±2	1±1	3.2±0.6	0.8±0.2
^{6}Li foil 40 μm	7±1	0.9±0.3	4.49±0.02	0.57±0.01
^{6}Li foil 70 μm	12±1	0.3±0.3	8.67±0.03	0.8±0.2

Also, it demonstrated the detection efficiency for neutron conversion (NC) events meeting energy discrimination criteria. The results are consistent with the others derived from the simulation which were mentioned in section 2. The detection efficiency is determined by subtracting the appropriate gamma-rays counting rate of the bare sensor from the total counting rate of the detector with ^{6}Li / ^{6}LiF converter in a sandwich configuration. Then, dividing this by the measured neutron flux at the calibration position.

4.2 Bare-sensor with no lithium converter.

The sensitivity of a Si wafer to gamma-ray is expected to be low for a thickness range of $30 - 300$ μm since the detection efficiency is close to 100 % for γ-ray energy of 10 keV, falling approximately to 1 % for 150 keV.[13] Therefore, Si sensor diode with a thickness of 300 μm is compatible with high background gamma rays. Also, This thickness is optimum to reduce electronic noise as the capacitance decreases as the thickness increases.

According to fig 4 which presents the measured energy spectra for both Am/Be neutron source and ^{60}Co gamma-rays source, all gamma-rays observed by the detector had a lower energy below 1 MeV. This deposited energy is less than the energy deposited by a neutron-induced a triton. This is particularly true for the ^{60}Co source which emits two gamma-rays of 1.17 and 1.33 MeV and even for the high energy gamma-rays of about 4.4 MeV from Am/Be neutron source.

The energy from these photons stored in the detector is still considerably less than that of 2.78 MeV triton which is deposited in this silicon sensors. Because these high energy gamma-rays can not be fully stopped by silicon sensor which has a light atomic number (Z=14) in addition to the very low thickness of this silicon sensors.

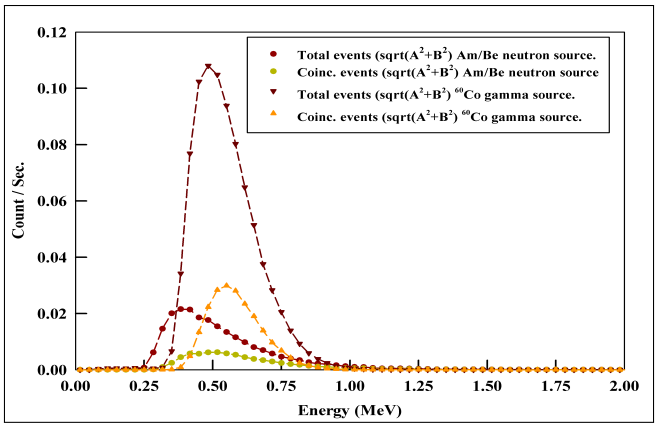

Fig 4. Bare sensors used for detection of gamma-rays from both Am/Be neutron source and ^{60}Co gamma source.

For a ^{60}Co source, based on the strength of the source and source−detector geometry, over the duration of the run, 1.51×10^{8} photons are incident on the detector. Hence, the gamma ray rejection ratio of the detector when using pulse-height discrimination is better than 10^{8} as presented in table 4.

Table 4. Measurements using ^{60}Co with activity 30 kBq, 2 cm distance from the sensor over a period of 252725 s.

	Total (A+B)	Coincidence	NC single events	NC coinc. events
Counts	215452	106394	11	1
count rate	0.853±0.002	0.421±0.001	$(4.4\pm1.3)\times10^{-5}$	$(4\pm4)\times10^{-6}$
$\gamma-$ray sensitivity	$(1.428\pm0.003)\times10^{-3}$	$(7.05\pm0.02)\times10^{-4}$	$(7.3\pm2.2)\times10^{-8}$	$(6.6\pm6.6)\times10^{-9}$

For the Am/Be neutron source, the approximate $\gamma-$exposure rate is 1 mR/h per 10^{6} n/sec. The computed flux per Ci of 4.43 MeV and 60 keV $\gamma-$ray for moderating water sphere of thickness 25 cm is approximately 5 and 2 photon/cm$^2/s$ respectively.[14] So, it is estimated that the total gamma-rays flux including a different rang of energies at 75 cm from the source, including the 25 cm of water is approximate, 10.5 gammas/cm$^2/s$.

Over the duration of the run, 1.85×10^{6} photons penetrate into the detector. However, over the entire run, no gamma radiation resulted in a neutron−like measurement based on the pulse height discrimination method used here, for single observed pulses or coincidences compared for the measurement of the bare sensor with ^{60}Co gamma source.

Consequently, whatever gamma radiation energy hits the detector it will deposit a small fraction of its energy or it could be fully absorbed in the detector after losing a great amount of its energy through many collisions with the surrounding. GAMBE thermal neutron detector achieves a high gamma-rays rejection factor of 10^{8}, so it could be used efficiently for the detection of thermal neutrons in high background gamma-rays filed.

4.3 Sandwich detector configuration with LiF film.

A ^{6}LiF film of thickness 7 μm in a sandwich detector configuration with two Si sensors with an active detection area of 1 cm^2 mounted in an aluminum testing box designed to eliminate photoelectric noise. This detector achieved a coincidence detection efficiency of 1 ± 1 % related to neutron events, and the total thermal neutron detection efficiency is 4 ± 2 %.

Figure 5 presents the energy spectrum related to the energy deposited by an alpha-triton pair in a silicon sensor using counts per second at different energies. Subtracting the energies stored by gamma rays does not affect the count rate for energies higher than 1 MeV. This energy spectrum shows that the highest count rate at 2.35 MeV is related to the triton particle with energy 2.73 MeV and the remaining counts below 1 MeV are approximately related to alpha particle.

A triton is more likely to traverse through ^{6}LiF layers than an alpha particle with energy 2.05 MeV. This shift in energy from 2.73 to 2.35 MeV is due to the amount of energy lost by the charged particle moving through a medium. The values of energy loss for the triton and alpha particle for 1 μg/mm^2 layer of ^{6}LiF are 21 keV and 130 keV respectively.[15]

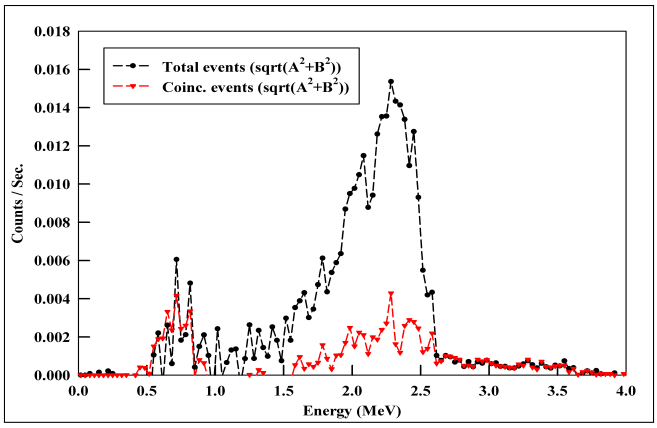

Fig 5. Counts rate of the GAMBE detector with ^{6}LiF film of 7 μm thickness for neutron detection from Am/Be neutron source.

4.4 Sandwich detector configuration with Li foil.

Results discussed here for a pure ^{6}Li foil of thickness 40 and 70 μm in the same sandwich detector configuration as ^{6}LiF film with two Si sensors with an active detection area of 1 cm^2. Nevertheless, ^{6}Li foil is mounted in an aluminum testing box which is designed and filled with an argon gas to protect ^{6}Li from corrosion due to its chemical reactivity.

According to both ^{6}Li foil thicknesses of 40 and 70 μm, the coincidence detection efficiency was varied from 0.9$\pm$0.3 % to 0.3$\pm$0.3 % and total detection efficiency from 7$\pm$1 % to 12$\pm$1 % respectively. These results show that the coincidence detection efficiency will be affected by the variation of the ^{6}Li foil thickness as it will be decreased as the thickness of foil increased. However, the total detection efficiency of the neutrons which induced single events will be increased.

Figure 6 presents the energy spectrum related to the energy deposited by alpha-triton pair in both silicon sensors using the same methodology which has been discussed before for a sandwich detector with a ^{6}LiF film. The count rate for events at energy lower than 1 MeV which still exists is entirely due to gamma rays because ^{6}Li has corroded due to its chemical reactivity. However, the chemical reactivity of pure ^{6}Li requires a cumbersome handling procedure. Lithium-6 in its pure metallic form is more recommended than ^{6}LiF compound because of its higher neutron detection efficiency.

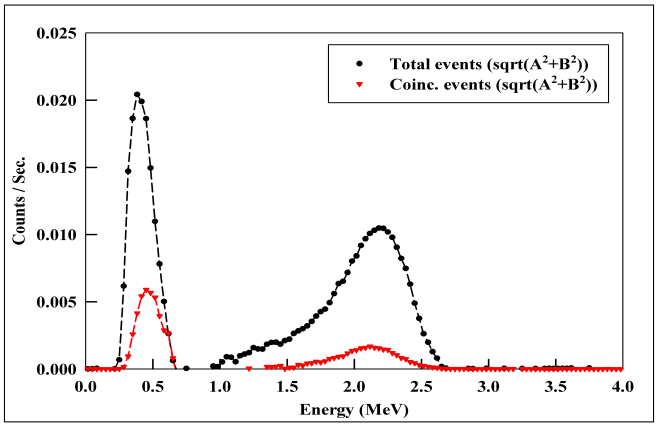

Fig 6. Counts rate of the GAMBE detector with ^{6}Li foil of 40 μm thickness for neutron detection from Am/Be neutron source.

5. CONCLUSION.

The practicability of using enriched ^{6}Li with silicon sensors in a sandwich configuration as a thermal neutron counter has been investigated. Tests have been performed using ^{6}Li as a ^{6}LiF coating and in its pure metallic form as a foil. Detector efficiency has been measured for both configurations when both reaction products are observed in coincidence related to neutron conversion events. For the ^{6}LiF configuration, the measured efficiency was 1 ± 1 % for 7 μm film and 0.9 ± 0.3 % for the ^{6}Li foil configuration of thickness 40 μm.

Detector efficiency has also been measured for both configurations when at least one of the reaction products (the triton) is detected. For the ^{6}LiF configuration of thickness 7 μm, the measured efficiency was 3.2 ± 0.6 % and for the ^{6}Li foil configuration of thickness 40 μm, the measured efficiency was 4.49 ± 0.02 %. The pulse height discrimination method outlined here was found to be very successful at rejecting gamma-rays, to be better than 10^8.

ACKNOWLEDGMENTS

Firstly, I would like to express my sincere gratitude to my supervisors Dr. H. van Zalinge, Dr. S. Burdin and Prof. G. Casse, for the continuous support and for their patience, motivation, and immense knowledge. In addition they provided me an opportunity to join their team as intern, and who gave access to the Liverpool semiconductor laboratory and research facilities. Without they precious support it would not be possible to conduct this research.

REFERENCES

[1] Caruso, A. N., "The physics of solid-state neutron detector materials and geometries," *Journal of Physics: Condensed Matter* **22**(44), 443201 (2010).

[2] Knoll, G. F., [*Radiation detection and measurement*], John Wiley & Sons (2010).

[3] Leroy, C. and Rancoita, P.-G., [*Principles of radiation interaction in matter and detection*], vol. 2, World Scientific (2009).

[4] Engels, R., Kemmerling, G., Nöldgen, H., and Schelten, J., "Thermal neutron detection with lithium-6 converters," **1**, 593–596 (2007).

[5] McGregor, D. S., Klann, R., Gersch, H., and Yang, Y., "Thin-film-coated bulk gaas detectors for thermal and fast neutron measurements," *Nuclear Instruments and Methods in Physics Research Section A: Accelerators, Spectrometers, Detectors and Associated Equipment* **466**(1), 126–141 (2001).

[6] McGregor, D. S., Klann, R. T., Gersch, H. K., and Sanders, J. D., "Designs for thin-film-coated semiconductor thermal neutron detectors," in [*Nuclear Science Symposium Conference Record (2001 IEEE)*], **4**, 2454–2458 (2001).

[7] McGregor, D. S., Gersch, H. K., Sanders, J. D., Klann, R. T., and Lindsay, J. T., "Thin-film-coated detectors for neutron detection," *Journal of the Korean Association for Radiation Protection* **26**, 167–175 (2001).

[8] Lutz, G. et al., [*Semiconductor radiation detectors*], vol. 10, Springer (1999).

[9] Guardiola, C., Fleta, C., Pellegrini, G., García, F., Quirion, D., Rodríguez, J., and Lozano, M., "Ultra-thin 3d silicon sensors for neutron detection," *Journal of Instrumentation* **7**(03), P03006 (2012).

[10] Petrillo, C., Sacchetti, F., Toker, O., and Rhodes, N., "Solid state neutron detectors," *Nuclear Instruments and Methods in Physics Research Section A: Accelerators, Spectrometers, Detectors and Associated Equipment* **378**(3), 541–551 (1996).

[11] McGregor, D. S., Hammig, M., Yang, Y.-H., Gersch, H., and Klann, R., "Design considerations for thin film coated semiconductor thermal neutron detectorsi: basics regarding alpha particle emitting neutron reactive films," *Nuclear Instruments and Methods in Physics Research Section A: Accelerators, Spectrometers, Detectors and Associated Equipment* **500**(1), 272–308 (2003).

[12] Agostinelli, S., Allison, J., Amako, K. a., Apostolakis, J., Araujo, H., Arce, P., Asai, M., Axen, D., Banerjee, S., Barrand, G., et al., "Geant4a simulation toolkit," *Nuclear instruments and methods in physics research section A: Accelerators, Spectrometers, Detectors and Associated Equipment* **506**(3), 250–303 (2003).

[13] Srivastava, S., Henry, R., and Topka, A., "Characterization of pin diode silicon radiation detector," *Journal on Intelligent Electronic Systems* **1**(1), 48 (2007).

[14] Gomaa, M., Henaish, B., and Ali, E., "Calculated neutron and gamma dose rates around a moderated am-be neutron source," *Applied Radiation and Isotopes* **44**(3), 638–640 (1993).

[15] Clements, P., "The calibration of ^{6}li semiconductor sandwich spectrometers," *Nuclear Instruments and Methods* **127**(1), 61–72 (1975).